Cellulose (2022) 29:8409–8425
https://doi.org/10.1007/s10570-022-04761-w

ORIGINAL RESEARCH

Study on spinnability of arabinoxylan extracted from barley husks

Svetlana Butylina · Krista Koljonen · Salla Hiltunen · Katri Laatikainen

Received: 28 December 2021 / Accepted: 14 July 2022 / Published online: 28 July 2022

Abstract Valorisation of bio-based materials derived from agricultural and industrial side-streams or waste-streams is a basis of circular economy. However, the success of it depends on the full understanding of materials and finding their optimal way of processing. Barley husk is a side-stream waste material derived from the starch and ethanol production. This study is focused on the processability of the arabinoxylan extracted from barley husk using the electrospinning technique to produce thin xylan-poly(vinyl alcohol) fibres. As a comparison, lignin-free xylan of beech wood was used. The properties of spinning solutions and resulting nanofibrous mats were assessed by using rheological measurements, FTIR spectroscopy, scanning electron microscopy and contact angle measurements. It was found that solubility plays a crucial role in the spinnability of xylan extracts. Decrease in viscosity of arabinoxylan achieved by decreasing its concentration was found to improve the jet stability but at the same time, to reduce the diameter of spun fibre. Hydrophilicity of nanofibrous mats were strongly affected by the type of xylan and solvent used. The xylan-based nanofibres have specific properties that could be used for developing value-added applications, such as material for scaffolds for tissue engineering, drug delivery, medical implants, biosensors, wound dressing, water filtration and packaging or further process into carbon nanofibres.

Graphical abstract

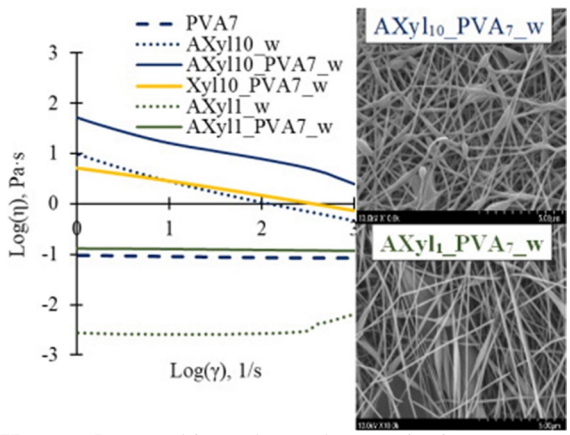

Keywords Arabinoxylan · Electrospinning · Nanofibres · Rheology · FTIR spectroscopy · Contact angle

Introduction

Circular economy has increased the usage of the biopolymers derived from various side streams and industrial waste materials both in agriculture and wood processing. The importance of circular

S. Butylina (✉) · K. Koljonen · S. Hiltunen · K. Laatikainen
Department of Separation Science, LUT School of Engineering Science, LUT University, Yliopistonkatu 34, 53850 Lappeenranta, Finland
e-mail: svetlana.butylina@lut.fi

economy in the fight against microplastic and carbon dioxide emissions has been well acknowledged in recent years (Forni 2020). Biopolymers originated from industrial and agricultural side streams can be divided into three groups such as polysaccharides (cellulose, hemicellulose, starch, chitin), proteins (silk, collagen) and phenol-based polymer lignin (Moohan et al. 2019). Hemicelluloses are of specific interest being a second most abundant group of biopolymers after cellulose and representing 30–40% of agricultural residues (Sun et al. 2011), but compared to cellulose, they have been barely utilized as raw material (Peng et al. 2014). Among all types of hemicelluloses, xylans are the most abundant type, which can be further divided into subclasses: homoxylans, glucuronoxylans, (arabino)glucuronoxylans, arabinoxylans, (glucurono)arabinoxylans and heteroxylans (Ebringerová 2006). The fractionation and purification of some specific xylans from plant-based materials is complicated, costly, and time-consuming process (Ferrari et al. 2015). Use of crude (non-refined) xylan-containing extracts wherever it is possible can significantly reduce the cost of product.

Increased interest in barley husks can be explained by significance of barley (*Hordeum vulgare*) as a crop plant. Finland produces barley in amount of 1.4 million tons per year (Luke 2020), whereas worldwide annual production is 160 million tons (FAO 2019). Husk is the outermost layer of the grain which forms 10–20% of the grain weight (Holopainen-Mantila 2015; Bhardwaj et al. 2020), and a side-stream waste material from the manufacture of starch and ethanol (Köhnke et al. 2009). Traditionally, barley husk has been peeled off and burned. Extraction method used can affect chemical composition of barley husk material (Höije et al. 2005, 2006; Börjesson 2018), however, mostly it consists of hemicelluloses, i.e. arabinoxylan, and cellulose with smaller amounts of lignin, protein, starch and fat. Recently, possibilities to exploit the fractions of barley husk in high-value product for different applications have been studied. Lähde et al. (2020) has described synthesis of nanostructured silicon carbide and graphene-like carbon from the silica extracted from barley husk. The transformation of cellulose fraction of barley husk into nanocellulose by sulphuric acid hydrolysis was studied by Börjesson et al. (2018). Höije et al. (2005) have published research on development of oxygen barrier coatings from arabinoxylans extracted of barley husks. Berglund et al. (2018) have studied the formation of composite aerogels from lignin-containing arabinoxylan and cellulose nanofibers which could be applied in the soft tissue engineering.

Electrospinning is a distinguished method for the preparation of nanofibres consisting of dissolved or melt polymers and biopolymers or their blends (Frenot and Chronakis 2003; Subbiah et al. 2005; Agarwal et al. 2009, 2016). In electrospinning process, a polymer solution or melt is placed into a syringe with a millimeter-size nozzle and is subjected to high electric field. Under the applied electrostatic force, the polymer is ejected from the nozzle and transported and deposited on a collector, which also serves as the ground for the electrical charges. Electrospun fibres have been widely used in several applications including scaffolds for tissue engineering, drug delivery, medical implants, biosensors, wound dressing (Rogina 2014), water filtration and packaging materials (Torres-Giner et al. 2018). Usually, the electrospun fibres have unique properties, such as high surface area-to-volume ratio, high pore interconnectivity and easy surface functionalization.

Several studies have been published on spinnability of various xylans. Krishnan et al. (2012) and Venugopal et al. (2013) have studied the beech-wood derived glucuronoxylan and Duan et al. (2019) have electrospun the arabinoglucuronoxylan extracted from straw fibres. In these studies, different solvents were used: 1 N sodium hydroxide and hot water, respectively. Most often, poly(vinyl alcohol) (PVA) and poly(ethylene oxide) (PEO) have been used to ensure the adequate entanglements and to facilitate the electrospinning of the xylan solutions. Due to the excellent properties of PVA, such as water-solubility, non-toxicity, biodegradability, it has been widely used in different nanofibre composite materials, for example, together with nanoclay (Ristolainen et al. 2006), chitosan (Park et al. 2009), aloe vera (Abdullah et al. 2014) and graphene oxide (Wang et al. 2012). Lignin has also been successfully electrospun with PVA (Ago et al. 2012). Additionally, the electrospun wheat xylan nanofibres (Duan et al. 2019) and also plant-based lignin (Kumar et al. 2019) have been processed further to fabricate carbon nanofibers.

Limited dispersion and solubilization of biopolymers are factors which make their electrospinning process challenging (Peresin and Rojas 2014). It has been shown in numerous studies (Ebringerová and

Heinze 2000; Ebringerová 2006; Glasser et al. 2000; Roos et al. 2009) that solubility of xylans and their rheological behaviour depend on their plant origin, molecular structure, and method of extraction. Therefore, solubility is one of the subjects which will be addressed in the present study.

Objective of this work was to produce arabinoxylan-based nanofibres focusing first on the different dissolving methods (water/alkaline) of arabinoxylan extract and then on the variables affecting the spinnability. The concentration of arabinoxylan in the arabinoxylan/PVA solutions was varied and surfactant addition was studied also. The properties of spun fibres were explained in terms of the physico-chemical characteristics (e.g., viscosity, conductivity, surface tension) of the solutions. Special attention was paid to the role of lignin in spinning of arabinoxylan extract. The xylan from beechwood was used as a reference. The quality of fibres was assessed by scanning electron microscopy and their chemistry was studied by FTIR spectroscopy and contact angle measurements. Based on the knowledge of the authors, this is the first time that arabinoxylan of barley husk with PVA has been electrospun into nanofibres.

Materials and methods

Material

The commercial grade poly (vinyl alcohol), PVA (Aldrich Chemistry), had a molecular weight of 89–98 kg/mol and 99% degree of hydrolysis. Arabinoxylan (AXyl) (Xylophane AB, Gothenburg, Sweden) was an extract from barley husk. According to the manufacturer specification, the sugar composition of this extract consisted of xylose (48.5%), arabinose (11.7%) and glucose (3.8%). The non-hemicellulose components of extract consisted of Klason lignin (19.6%), fat (4.2%), ash (4.3%) protein (6.8%) and starch (less than 1%). The molar mass of arabinoxylan was 34 kg/mol (Gröndahl et al. 2014). European beechwood xylan was pharmaceutical grade (Iris Biotech GmbH) consisting of poly(beta-D-xylopyranose [1→4]) linkages. According to the size-exclusion chromatography analysis conducted by manufacturer, the molar mass (M_w) of beechwood xylan was 13.24 kg/mol. Both, the barley husk xylan and the beechwood xylan were used without further treatment. Benzalkonium chloride, BAC, (Fluka ≥ 95.0%) was used as a cationic surfactant. It contained $H_2O \leq 10\%$ and ash as $SO_4 \leq 0.1\%$ and was a mixture of 60% C_{12} and 40% C_{14} homologues. The average molar mass of BAC was 350 g/mol and critical micelle concentration (CMC) was 3 mM determined in 0.1 mM NaCl (Turku and Sainio 2009).

Methods

Preparation of spinning solutions

Two types of approach were used to dissolve xylan, referred in this study as Method A and B. In the Method A described by Duan et al. (2019), the xylan powder is dissolved in water under vigorous magnetic stirring at 80 °C for 24 h in tightly sealed flask as illustrated in Fig. 1. Thereafter, the 7 g of PVA powder was added into prepared solution and heated at 80 °C under stirring at 500 rpm for 3 h to complete the dissolution of PVA followed by the overnight stirring without heating. The 10 mmol of cationic surfactant, benzalkonium chloride (BAC) was added to the $AXyl_1\_PVA_7$ solution and thoroughly stirred overnight.

In Method B shown in Fig. 1, the arabinoxylan powder was dissolved in 1 N NaOH solution and mixed for 24 h at room temperature. The 7 g of PVA was added using the same procedure as in Method A. The composition of the spinning solutions, including type of xylan used, solvent, content of components and final spinning dope concentration have been summarized in Table 1. The final spinning dope concentration was calculated using formula:

$$C_{spinning\ dope} = \frac{\left(m_{xylan} + m_{PVA}\right)}{\left(m_{xylan} + m_{water} + m_{PVA}\right)} \times 100(\text{wt.\%})$$

where m_{xylan}, m_{water} and m_{PVA} are the masses of xylan, water and PVA added to solution.

Analyses applied to characterize spinning solutions

Rheological properties of the solutions were measured using Anton Paar Modular Compact Rheometer MCR 302 equipped with concentric cylinder CC27 system at temperature of 20 °C. The pHs and conductivities of the solutions were determined with the multi parameter meter (VWR MU 6100L). The

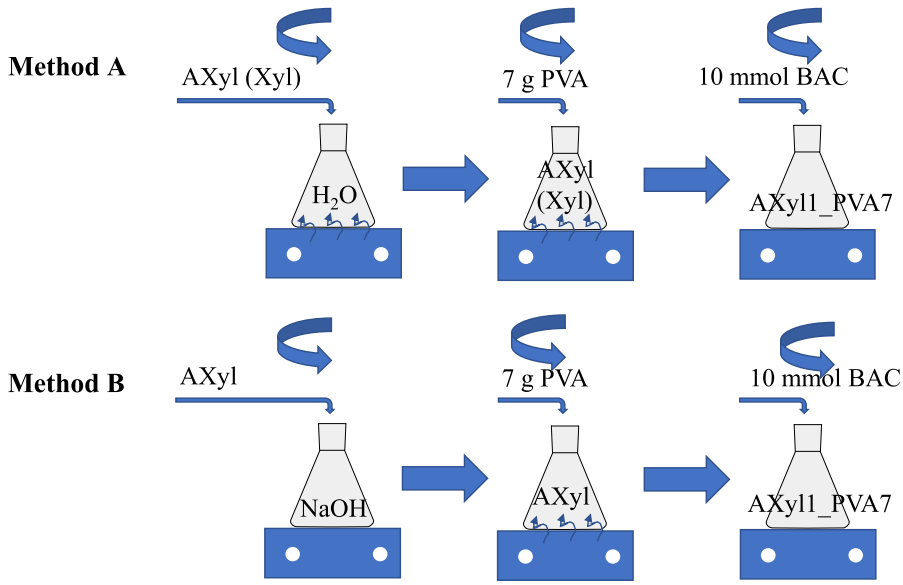

Fig. 1 Schematic representation of preparation procedure of xylan (arabinoxylan, AXyl, and xylan, Xyl) and PVA solutions referred as Methods A and B using two types of solvent: water, and sodium hydroxide, respectively. Cationic surfactant (benzalkonium chloride, BAC) was added in the final stage

Table 1 Composition of the solutions used in electrospinning

Spinning solution	Type	Xylan Content (wt.%)	Solvent	PVA (g)	Final spinning dope conc. (wt%)	Surfactant (mmol)
Xyl_{10}_PVA_7_w	Xylan	10	H_2O	7	15.9	
$AXyl_{10}$_PVA_7_w	Arabinoxylan	10	H_2O	7	15.9	
$AXyl_{2.5}$_PVA_7_alk	Arabinoxylan	2.5	1 N NaOH	7	8.9	
$AXyl_1$_PVA_7_alk	Arabinoxylan	1	1 N NaOH	7	7.5	
$AXyl_1$_PVA_7_alk_BAC	Arabinoxylan	1	1 N NaOH	7	7.5	10
$AXyl_1$_PVA_7_w	Arabinoxylan	1	H_2O	7	7.5	
$AXyl_1$_PVA_7_w_BAC	Arabinoxylan	1	H_2O	7	7.5	10

surface tension was measured by the Du Nouy Ring method using a platinum ring and surface tension tester (Krüss GmbH, Hamburg, Germany).

Electrospinning

Electrospinning was performed using a modular bench top Spinbox instrument (Bioinicia, Valencia, Spain). The distance between nozzle and collector plate was 13 cm, and pumping speed was 0.3 mL/h. The current applied varied from 25 to 12 kV depending on the composition (conductivity) of the electrospun solution. The relative humidity inside the chamber varied from 27 to 41% depending on the day of the measurement.

SEM Hitachi SU3500 scanning electron microscope was applied to analysed gold-coated samples. Images were taken at the accelerated voltage of 10 kV using various magnifications: 1000 × and 10,000x. Diameters of spun fibres were analysed using ImageJ software. At least 100 fibres were measured to determine the mean diameter and standard deviations.

FT-IR analysis

A PerkinElmer FT-IR Spectrometer Frontier equipped with ATR sampling accessory was used to acquire spectra of electrospun mats. Spectra were recorded in the range of 4000 to 400 cm^{-1} at resolution 4 cm^{-1}. Each spectrum consisted of 10 scanning runs.

Contact angle measurements

The contact angles of the electrospun mats were measured using a sessile drop test method. The electrospun mat was fixed on the sample glass with double-sided tape in order to obtain as smooth surface as possible. 10 µL of deionised water was placed on the surface of the sample by syringe and three images were immediately taken by camera and handled using CAM 2008 software (KSV instruments, Finland). Out of the three images, the software calculates the contact angles of the water drop on the surface. At least 5 different locations were measured per each mat.

Results and discussion

Electrospinning of Xyl_{10}_PVA_7_w and $AXyl_{10}$–PVA_7_w solutions prepared using method A

In Method A, hot water (80 °C) was used to prepare 10 wt% xylan (Xyl and AXyl) solutions according to the procedure described by Duan et al. (2019). At 10 wt% concentration, the beechwood xylan powder was soluble in hot water at 80 °C, whereas the barley husk xylan powder formed a dispersion. Indeed, xylans isolated from biomass are known to have poor solubility in aqueous and aprotic solvents (Jain et al. 2001). PVA concentration of 7 wt% was chosen based on the preliminary electrospinning trials and easy spinnability at room temperature. Increase in PVA concentration to 10 wt% resulted in formation of thick gel in the syringe.

In general, no disturbances in flow coming from nozzle (so-called, Taylor cone) were observed during spinning of the solution containing beechwood xylan and PVA mixture. The SEM images of the electrospun mat containing beechwood xylan (10 wt%) and PVA (7 wt%) have been shown in Fig. 2. The Xyl_{10}–PVA_7_w electrospun mat had a homogeneous physical appearance. However, SEM images (Fig. 2, right) show that nanofibers were containing inclusions such as local thickenings (knots) and beads.

In the case of the $AXyl_{10}$_PVA_7_w solution prepared by Method A, separation of flow coming from the nozzle into white and dark brownish parts became evident immediately after the formation of Taylor cone. More continuous colourless part of the flow resulted in the white or slightly beige mat on the collector plate, which was interrupted by the dark brownish part as shown in Fig. 3. The brownish part flied to collector plate in the form of droplets. Some of these brownish droplets were falling under gravity force in the interspace between nozzle and collector. Several attempts were made to increase the electrostatic force, for example, by increasing voltage and by reducing distance between nozzle and collector plate to minimum. However, it was impossible to overcome the effect of the gravitational force.

The morphology of the $AXyl_{10}$_PVA_7_w mat was studied using SEM analysis and the images have been shown in Fig. 4. A typical morphology of brownish droplets is indicated with boundary line in Fig. 4

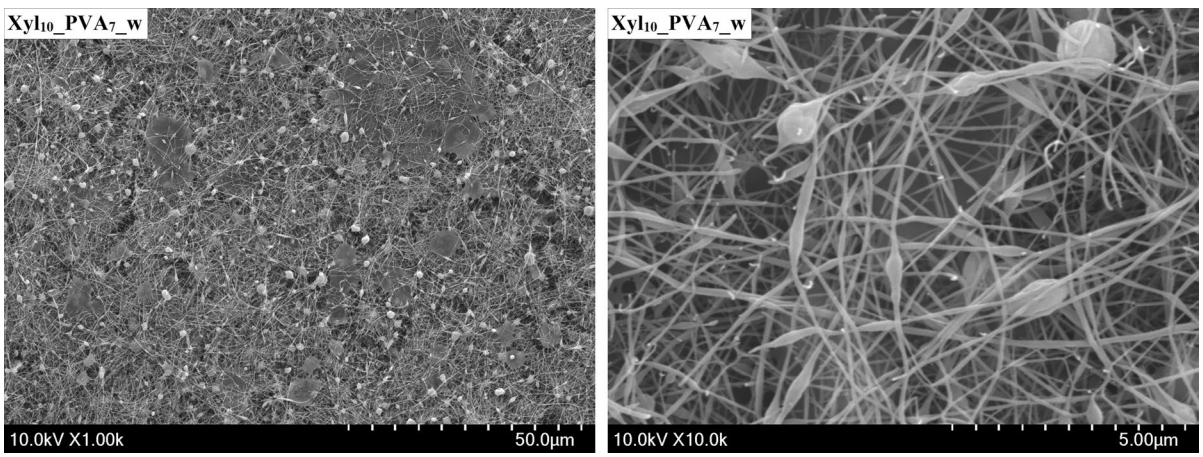

Fig. 2 SEM images of Xyl_{10}_PVA_7_w fibres: magnification 1000x (left) and 10,000x (right)

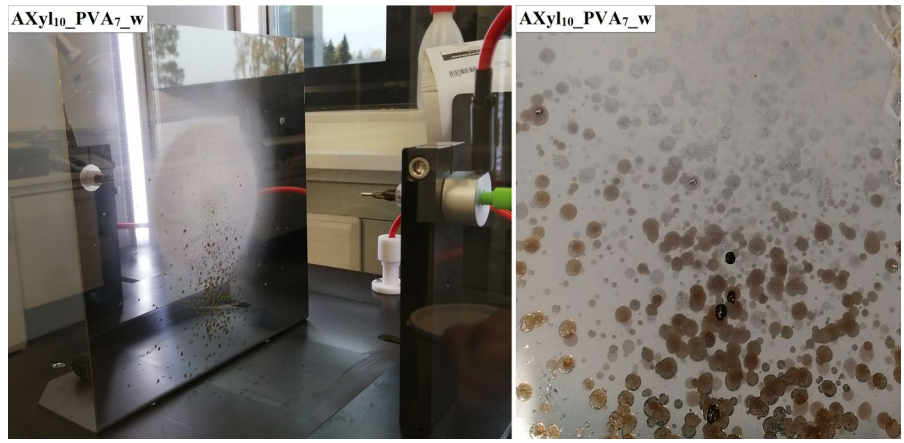

Fig. 3 Formation of white and brownish parts during electrospinning of $AXyl_{10}$–PVA_7_w solution

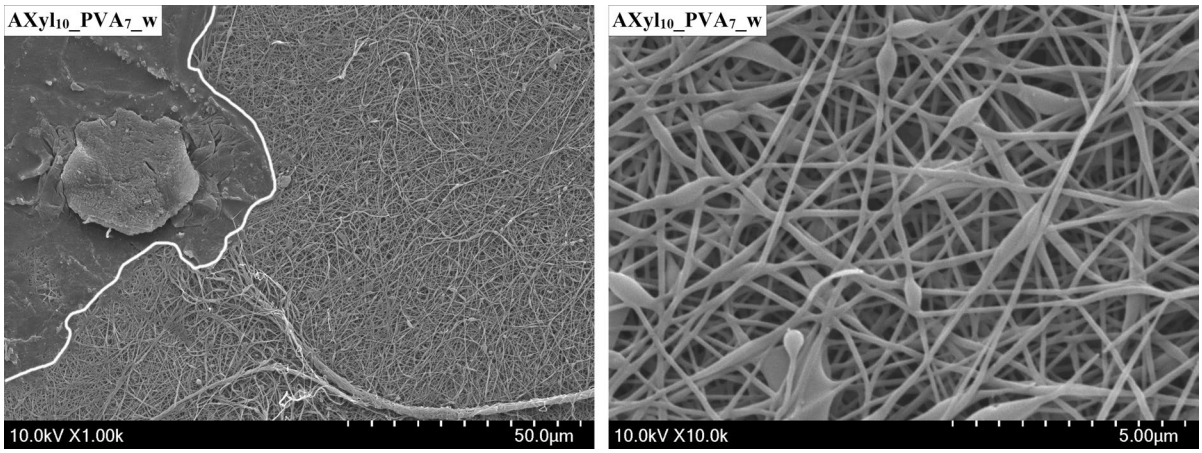

Fig. 4 SEM images of $AXyl_{10}$_PVA_7_w fibres obtained as different magnifications: 1000x (left) and 10,000x (right)

(left) showing as fibreless spot. Instead, the fibrous part of the $AXyl_{10}$_PVA_7_w electrospun mat was containing inclusions, such as local fiber thickenings and large fibre joints which are visible in Fig. 4 (right).

Electrospinning of arabinoxylan/PVA solutions prepared using method B

During electrospinning of the $AXyl_{10}$_PVA_7_w solution, it was clear that phase separation in PVA-rich phase and hemicellulose-rich phase was taken place. Most probably, the insolubility of arabinoxylan extract in water was the main reason for flow instability. After a careful literature review on electrospinning of hemicelluloses, it was decided to use 1 N NaOH solution to dissolve arabinoxylan and decrease the concentration to 2.5 wt%. While the flow of $AXyl_{2.5}$_PVA_7_alk solution was improved compared to $AXyl_{10}$_PVA_7_w solution, the formation of droplets caused by flow instabilities was still noticeable. The electrospun fibres have been shown in Fig. 5. The thickest fibres of the study were spun from $AXyl_{2.5}$–PVA_7_alk solution (Fig. 5, right).

In order to improve flow, the further decrease of arabinoxylan content and addition of the cationic surfactant were implemented. SEM images of the electrospun fibres have been shown in Figs. 6 and 7. As expected, both decrease in the arabinoxylan concentration and the addition of the cationic surfactant, benzalkonium chloride, resulted in improvement of the flow of the solution used in electrospinning and, simultaneously, the quality of the electrospun mat. Moreover, comparison of mats in Figs. 5, 6 and 7 and results shown in

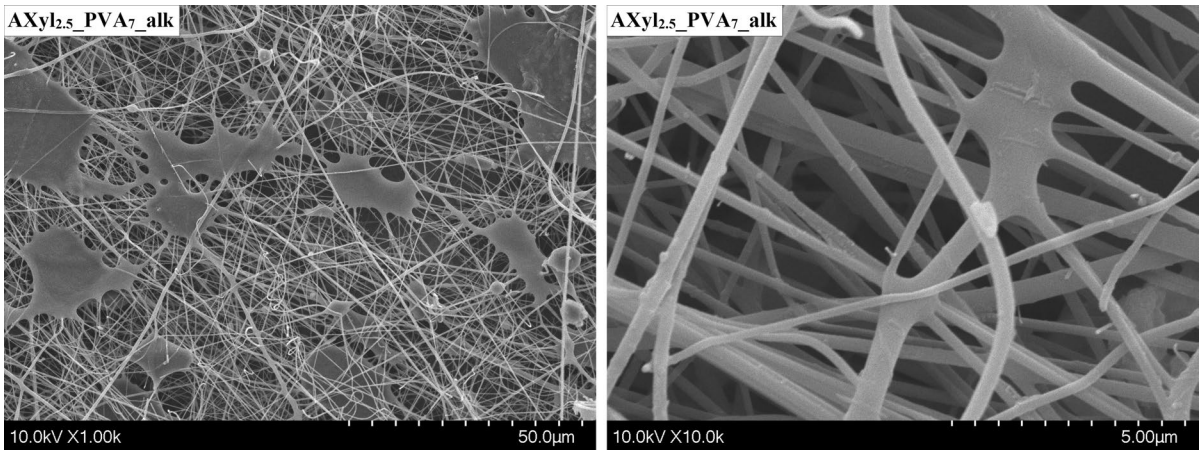

Fig. 5 SEM images of $AXyl_{2.5}\_PVA_7\_alk$ fibres at magnifications: 1000x (left) and 10,000x (right)

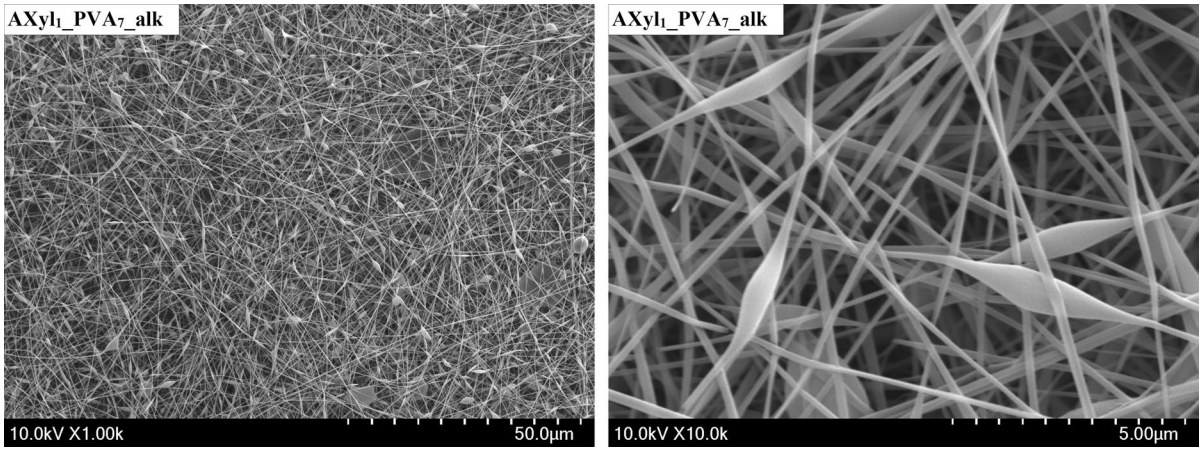

Fig. 6 SEM images of $AXyl_1\_PVA_7\_alk$ fibres at magnifications: 1000x (left) and 10,000x (right)

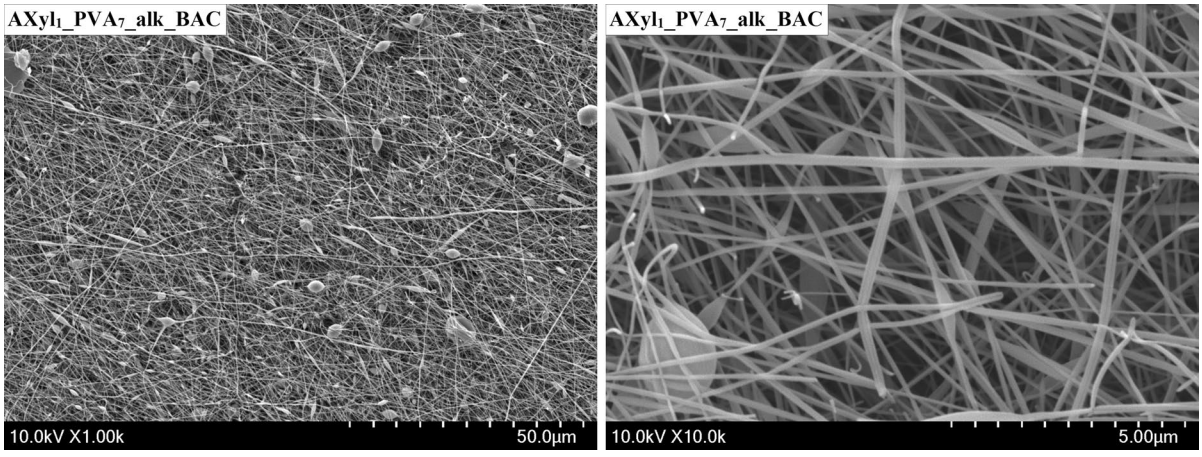

Fig. 7 SEM images of $AXyl_1\_PVA_7\_alk\_BAC$ fibres at magnifications: 1000x (left) and 10,000x (right)

Table 2 Calculated diameters and defects of fibres

Sample	Diameter of fibres (nm)	Size of defects (nm)
PVA_7_w	148.0 ± 39.2	> 300
Xyl_{10}_PVA_7_w	100.5 ± 39.5	< 300
$AXyl_{10}$_PVA_7_w	146.8 ± 53.1	> 300
$AXyl_{2.5}$_PVA_7_alk	212.3 ± 55.7	> 300
$AXyl_1$_PVA_7_alk	156.3 ± 43.0	> 300
$AXyl_1$_PVA_7_alk_BAC	121.2 ± 36.5	> 200
$AXyl_1$_PVA_7_w	130.5 ± 35.0	< 250
$AXyl_1$_PVA_7_w_BAC	75.7 ± 29.8	> 200

Table 2 revealed that the electrospun mat containing cationic surfactant was composed by the thinner fibres and had the denser structure compared to the others. Nevertheless, the large fiber joints were not found in mats consisting of $AXyl_1$_PVA_7_alk (Fig. 6, right) and $AXyl_1$_PVA_7_alk_BAC (Fig. 7, right). None of the applied strategies, however, led to the complete disappearance of defects such as beads and local fibre thickenings. According to the results obtained by Lee et al. (2003) in their study on electrospinning of polystyrene fibres, beads in electrospun fibres are inevitable with below 15 wt% solutions of polystyrene. The morphology of beads has been found to depend on polymer concentration, applied voltage and nozzle-to-collector distance.

Electrospinning of $AXyl_1$_PVA_7 solutions prepared by method A with and without surfactant

There was also an interest to see if by applying similar strategy, i.e., decrease in hemicellulose concentration (i.e., from originally used 10 wt% to 1 wt%) and addition of cationic surfactant will lead to improvements in the case of water-based solution of arabinoxylan. Analysis of SEM images of $AXyl_1$_PVA_7_w and $AXyl_1$_PVA_7_w_BAC mats shown in Fig. 8 and Fig. 9 revealed trends similar to ones found for alkali-dissolved xylan with PVA ($AXyl_1$_PVA_7_alk) and with cationic surfactant ($AXyl_1$_PVA_7_alk_BAC) containing mats (shown in Figs. 6 and 7). The electrospun mats were more uniform compared to the initial $AXyl_{10}$_PVA_7_w mat (Fig. 4) and fibres were finer. Somehow, the exchange of alkali to water led to the denser structure of the resulting mat.

Size of electrospun fibres

Average diameters of the fibres in the structure of the electrospun mats were calculated using Image J software and the results have been presented in Table 2. Results shown in the Table 2 are average of calculations made for 100 fibres per each type of mat. The 7% aqueous solution of PVA spun at pumping rate of 0.3 mL/h, distance of 13 cm, voltage of 20 kV was used as a reference. From Table 2 it is evident that solution containing xylan extracted from beechwood, Xyl_{10}_PVA_7_w, resulted in finer fibres than solution containing arabinoxylan

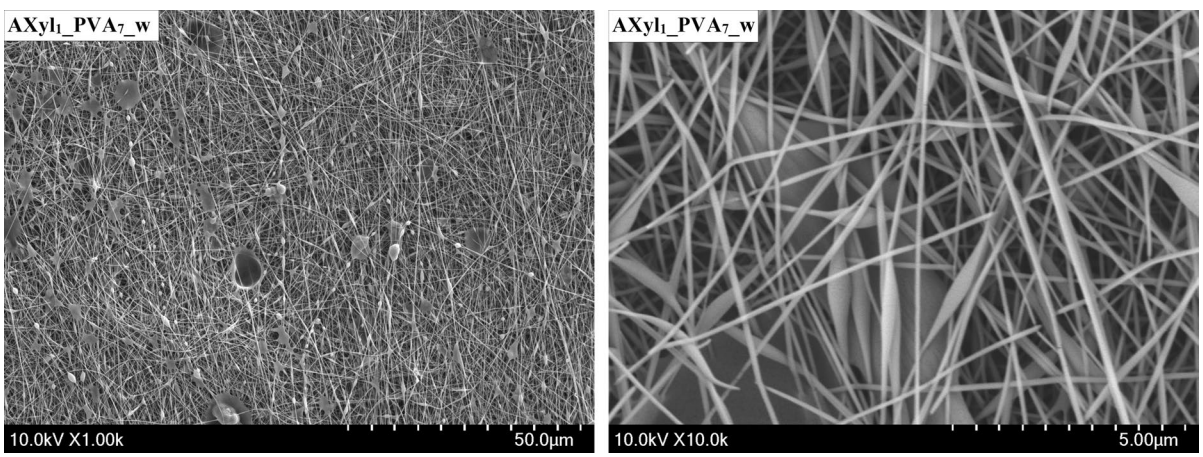

Fig. 8 SEM images of electrospun $AXyl_1$_PVA_7_w mats without cationic surfactant: 1000x (left) and 10,000x (right)

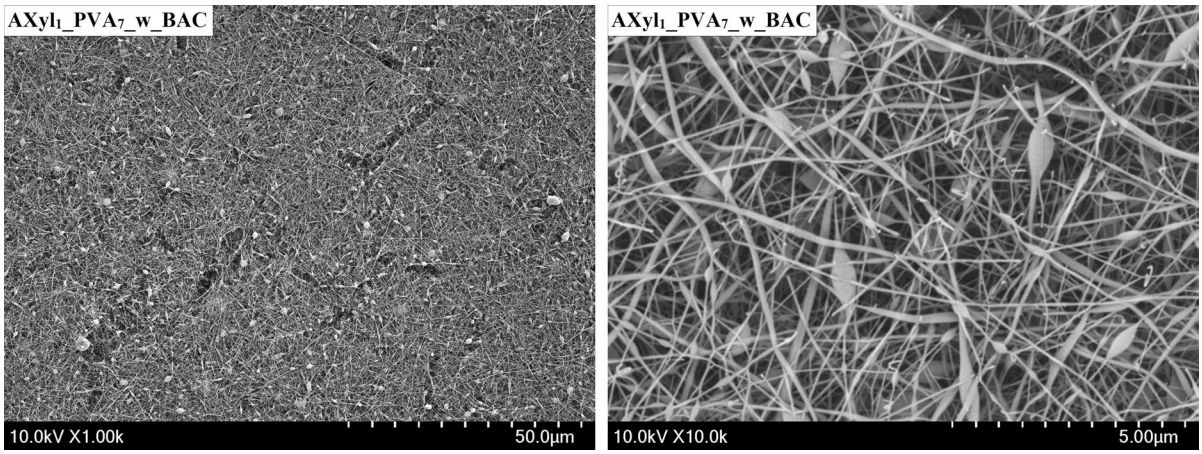

Fig. 9 SEM images of electrospun $AXyl_1\_PVA_7\_w$ mats with cationic surfactant: 1000x (left) and 10,000x (right)

extracted from barley husks, $AXyl_{10}\_PVA_7\_w$. Operating conditions during spinning were identical for both types of xylan. Similarity between fibre size of PVA_7_w and $AXyl_{10}\_PVA_7\_w$ mats and flow (phase) separation observed in the case of the $AXyl_{10}\_PVA_7\_w$ solution electrospinning can indicate that the fibre mat consisted mostly of PVA while arabinoxylan was disposed as droplets. Chemical composition of the two phases and the results of the FTIR analysis of the mats will be discussed in the following section. Generally, the mats spun from the aqueous solutions had thinner fibres than their analogues spun from the alkaline solutions. Moreover, both the decrease in concentration of arabinoxylan from 2.5 to 1.0 wt% and use of cationic surfactant resulted in thinner fibres. More specifically, the 42% decline in the fibre diameter was calculated after addition of cationic surfactant to $AXyl_1\_PVA_7\_w$ solution.

Effects of solution properties on spinnability and appearance of the fibres

The appearance of the fibres collected depended on many factors (Jarusuwannapoom et al. 2005). One of them is the viscoelastic force, which depends on the concentration of the solution, average molecular weight of the polymer, viscosity, and surface tension of the solution. Another one is the gravitational force which depends on the density and the conductivity of the solution and electrostatic forces. Recognising this, conductivity, viscosity, and surface tension of solutions were measured, and results have been shown in Table 3. The solution conductivity is known to be one of the main parameters in the electrospinning process since the viscous polymer solution is stretched due to repulsion of the charges present on its surface. As expected, presence of sodium hydroxide drastically increased the conductivity of the solutions. Increased

Table 3 pH, conductivity, shear viscosity and surface tension of the xylan_PVA solutions

Sample	pH	Conductivity (mS/cm)	Shear viscosity[1] (Pa·s)	Surface tension, γ (mN/m)
$Xyl_{10}\_PVA_7\_w$	7.9	2.53	2.03	> 80
$AXyl_{10}\_PVA_7\_w$	8.7	1.29	11.33	55.3
$AXyl_{2.5}\_PVA_7\_alk$	13.3	54.10	0.55	42.8
$AXyl_1\_PVA_7\_alk$	13.2	57.37	0.25	41.9
$AXyl_1\_PVA_7\_alk\_BAC$	13.1	57.00	0.31	37.5
$AXyl_1\_PVA_7\_w$	7.0	0.63	0.12	49.0
$AXyl_1\_PVA_7\_w\_BAC$	6.5	1.17	0.11	37.0

[1] Shear viscosity was determined at shear rate of 50 1/s

conductivity resulted in decrease of voltage at which Taylor cone is formed (e.g., voltage decreased from 25 to 20 kV for the $AXyl_1$_PVA_7_w and $AXyl_1$_PVA_7_alk solution, respectively). However, high conductivity is not always guarantee spinnability of the solution. For example, solution of $AXyl_{10}$_PVA_7_w had higher conductivity than $AXyl_1$_PVA_7_w solution but its spinnability was problematic due to extremely high viscosity. Viscosity curves of the solutions as a function of shear stress including 10 and 1 wt% AXyl_w, 2.5 and 1 wt% AXyl_alk and 7 wt% PVA, are shown in Fig. 10.

Both xylans used, beechwood (Xyl) and barley husk (AXyl), contains of 4-O-methyl-glucuronic acids (Köhnke et al. 2009; Teleman et al. 2002), and, thus, they are negatively charged in aqueous solutions. Dissolution of the negatively charged groups is highly dependent on pH (Sjöström 1989). In the solutions studied (Table 3), these uronic acid groups are known to be fully dissociated at pH 6–8.5. At higher pH values when pH exceeds 12, also carbonyls and phenolic hydroxyl groups have been fully dissociated. According to manufacturer, arabinoxylan of barley husk contains lignin (Klason lignin 19.6%) bound to xylan, thus, it contains these phenolic hydroxyl groups. At pH 13, only small amount of hydroxyl groups in alcohols have reported to be dissociated (Sjöström 1989). Comparison of conductivity of $AXyl_{10}$_PVA_7_w and Xyl_{10}_PVA_7_w solutions shown in Table 3 indicates that Xyl contains higher charge (higher amount of 4-O-methyl glucuronic acid) compared to AXyl. In Table 3, increase of the pH up to 13 shows clearly that conductivity increase drastically showing increase of Na^+ an OH^- ions and possible increase of the dissociating groups.

When cationic surfactant, i.e. benzalkonium chloride, is added, complexation of charges between xylan and surfactant is evident. The driving force for the complexation between oppositely charged polyelectrolytes and surfactants are electrostatic

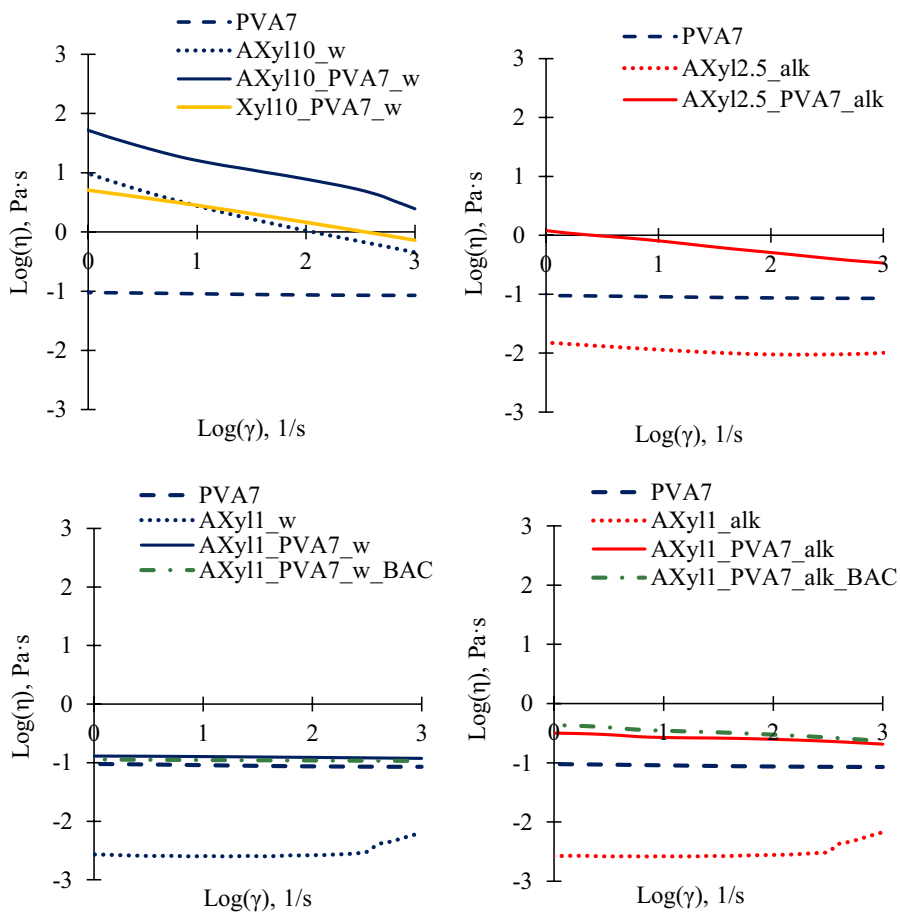

Fig. 10 Viscosity as a function of shear rate curves in a log–log representation

and hydrophobic forces (Holmberg et al. 2002). The head groups of the surfactant molecules are attracted by the charged polymer segments, and also the hydrophobic surfactant tails can interact with the hydrophobic backbone of the polyelectrolytes, such as lignin attached to xylan in AXyl. According to Table 3, surface tension of the solutions decreases from 41.9 to 37.5 (pH 13) and 49.0 to 37.0 (pH 6.5), respectively. Concentration of 10 mM for cationic surfactant (BAC) was used in the solutions, which is higher than the critical micelle concentration (CMC) of BAC reported, 3 mM (Turku and Sainio 2009). Schematic plot of the concentration dependence of the surface tension for mixed polymer solution described by Holmberg et al. (2002) shows that in the concentration of benzalkonium chloride used in the studies, CMC and critical association concentration CAC have been reach and micelles of surfactant have been formed, seen as lowered surface tension values of the solutions. Maximum effectiveness of benzalkonium chloride have been reported to exist between pH 4–10 (Handbook of Pharmaceutical Excipients 2006), indicating that the at pH 13 the quaternary ammonium compounds are not fully dissociated. Because PVA is also present in the solutions, the behavior of surfactant-polymer aggregations becomes more complex, which needs to be studied further.

Viscosity as a function of shear rate expressed as log (η) v's log (γ) for different spinning and reference solutions were shown in Fig. 10. As indicated in Fig. 10, viscosities of AXyl(Xyl)_PVA solutions decreased with increasing shear rate, indicating a shear-thinning or non-Newtonian flow behaviour. This non-Newtonian behaviour was characteristic especially for solutions having high content of polysaccharides (xylans). Viscosities of the reference solutions including 1 wt% AXyl (both aqueous and alkaline), 7 wt% PVA, and $AXyl_1\_PVA_7$ solutions were less dependent on shear rate.

The power-law model was applied to evaluate relation between viscosity and shear rate. The viscosity of a power law fluid changes proportionally to $K{\cdot}\gamma^{n-1}$, where K is the flow consistency index and n is the flow behaviour index (Mewis and Wagner 2011).

As shown in Table 4, the consistency index, *K* gradually decreases as the content of arabinoxylan decreases. This is seen especially in the case of reference arabinoxylan solutions (e.g., 8.068 v's 0.002 for 10 wt% and 1 wt% of AXyl_w, respectively), and in the case of AXyl_PVA solutions (e.g., 44.11 v's 0.157 for $AXyl_{10}\_PVA_7\_w$ and $AXyl_1\_PVA_7\_w$, respectively). At the same time, the flow behaviour index, *n,* increases and becomes closer to 1. In more detail, the $n \approx 1$ indicates near-Newtonian flow behaviour, while $n < 1$ indicates flow behaviour of pseudoplastic fluid. Among solutions studied, 7 wt% PVA and 1 wt% AXyl solutions showed behaviour close to Newtonian in wide range of shear stresses. As was discussed earlier, 7 wt% PVA solution was easily spinnable at ambient temperature. Thus, electrospinning solutions having viscosities close to viscosity of pure PVA 0.08 Pa·s (e.g., $AXyl_1\_PVA_7\_w$ and $AXyl_1\_PVA_7\_alk$ with and without surfactant) had good spinnability. According to results of rheological measurements not shown here, viscosity of the $AXyl_{10}\_PVA_7\_w$ and $AXyl_{2.5}\_PVA_7\_alk$ solutions made at higher temperatures (i.e., 50 and 80 °C) was drastically reduced. It was therefore concluded that decrease in the viscosity of the solution is considered as an efficient way to improve the spinnability.

Table 4 Rheological parameters of solutions studied evaluated according to power law equation

Sample	n	K	R^2
$Xyl_{10}\_PVA_7\_w$	0.717	5.322	1
$AXyl_{10}\_PVA_7\_w$	0.609	44.11	0.995
$AXyl_{2.5}\_PVA_7\_alk$	0.813	1.206	1
$AXyl_1\_PVA_7\_alk$	0.944	0.316	1
$AXyl_1\_PVA_7\_alk\_BAC$	0.914	0.434	1
$AXyl_1\_PVA_7\_w$	0.976	0.157	1
$AXyl_1\_PVA_7\_w\_BAC$	0.993	0.113	1
$AXyl_{10}\_w$	0.567	8.067	0.996
$AXyl_1\_w$	1.082	0.002	0.993
$AXyl_1\_alk$	1.089	0.002	0.994
PVA_7	0.982	0.095	1

The consistency index, *K,* is an indicator of the viscous nature of the system. The consistency index of the $AXyl_{10}\_PVA_7\_w$ solution was significantly higher compared to the $Xyl_{10}\_PVA_7\_w$ solution. Since equal amount of PVA was used in both solutions, the difference seen was connected to the nature of xylan. Both chemical composition and molecular mass of xylan can be a reason for that. Molar mass of the xylan extracted from beechwood ($M_w = 13.24$ kg/mol) is lower than molar mass of arabinoxylan extracted from barley husk (34.00 kg/mol). Chemical

compositions of xylan and arabinoxylan extracts will be discussed later.

Addition of PVA in AXyl solutions increased their viscosities (consistency indexes). This effect was independent on the concentration or alkalinity of the AXyl solution. Increase in the viscosity of two-component mixture may signify the polymer's interactions (or formation of larger particulates). Addition of PVA caused formation of hydrogen bonds between hydroxyl groups of PVA and of arabinoxylan and lignin molecules in arabinoxylan-lignin complex, and as a consequence, increased the viscosity of the solution. Lignin is supposed to be closely bound (in non-dissociated complex) to arabinoxylan in aqueous dispersion of barley husk extract. Indeed, a single step extraction, which commonly has been used to isolate xylan from barley husks (Glasser et al. 2000) resulted in xylan entrapped with lignin. According to the information available, 16-h extraction with 4 wt% sodium hydroxide solution at room temperature was applied to the dry cake of barley husks (Nygren 2009). Three types of linkages are known to exist between lignin and polysaccharides in lignin-carbohydrate complexes (LCC), i.e., benzyl ester-, benzyl ether- and glycosidic linkage, however only ester type is readily hydrolysed in alkali (Lai 1991).

The consistency index of the $AXyl_1$_PVA_7_w solution was lower compared to the $AXyl_1$_PVA_7_alk solution (e.g., 0.157 v's 0.316). The difference in viscosity could be explained by difference in chemical structure of arabinoxylan extract. Combination of alkali with heat treatment (i.e., at 80 °C for 3 h) used to prepare AXyl_PVA_alk solutions might lead to hydrolysis of the glycosidic linkages between lignin and arabinoxylan, which resulted in release of new phenolic hydroxyl groups of lignin (Lai 1991). Shifts associated with phenolic hydroxyl groups were identified in the FT-IR spectra of the electrospun AXyl_PVA_alk mats. These new phenolic hydroxyl groups and the arabinoxylan released can participate into formation of additional hydrogen bonds with PVA. It was suggested to be a reason for increased viscosity of $AXyl_1$_PVA_7_alk solution.

Increase in viscosity (consistency index) was found also in the case of addition of surfactant to alkaline $AXyl_1$_PVA_7 solution. A strong polymer-surfactant interaction could alter the rheological properties of the polymer solution, e.g., if the polymer can associate with the surfactants (Lin et al. 2004). In alkaline $AXyl_1$_PVA_7 solution, an addition of cationic surfactant is assumed helping to form large associates between positively charged micelles of surfactant and negatively charged groups of arabinoxylan and lignin. It was very interesting to note a difference in effects caused by surfactant on viscosities of $AXyl_1$_PVA_7_w and $AXyl_1$_PVA_7_alk solutions. Viscosity of $AXyl_1$_PVA_7_w_BAC solution was lower compared to the $AXyl_1$_PVA_7_w solution, in contrast to $AXyl_1$_PVA_7_alk_BAC solution. The difference can be explained by the difference in the dissolution state and by the charge of the arabinoxylan in pH-neutral and alkaline solutions. Most probably, at neutral pH there was not enough anionic groups in arabinoxylan/lignin-PVA complex available to participate into electrostatic interactions with benzalkonium cations associated in micelles. Formation of free micelles non-bound electrostatically to the polymer backbone, can be responsible for decrease in viscosity in the case of $AXyl_1$_PVA_7_w_BAC solution. However, this question requires more detailed study.

Surface tension of the solution is the factor, which can affect the spinnability. According to the Taylor equation, there is a relationship between voltage applied and the surface tension of the solution:

$$\left(\frac{V_c}{H}\right)^2 = \frac{4}{L^2}\left(\ln^2\frac{L}{R} - \frac{3}{2}\right)(0.117\pi\gamma R)$$

where V_c is the critical electrical voltage, H is the separation between the tip of nozzle (capillary) and collector plate, L is the length of the capillary, R is the radius of the capillary and γ is the surface tension of the solution (Yao et al. 2003). Voltage required to obtain a stable Taylor cone in a solution with or without cationic surfactant at the same working distance and pumping feed rate was noticeable different. Addition of cationic surfactant clearly reduced the surface tension of $AXyl_1$_PVA_7_alk and $AXyl_1$_PVA_7_w on 10.5 and 24.5% (Table 3), respectively, and, as consequence, resulted in lower applied voltage.

There is a strong connection between polymer concentration and thickness of fibres. As was discussed earlier, the average thickness of $AXyl_{2.5}$_PVA_7_alk fibres was higher than thickness of $AXyl_1$_PVA_7_alk fibres (212.3 ± 55.7 v's 156.3 ± 43.0 nm) (Table 2). The decrease in thickness of fibres with the decrease of polymer concentration was previously described by researchers using polystyrene (Uyar and Besenbacher

2008; Lee et al. 2003). Most often, high polymer concentration means higher viscosity. According to the studies on polystyrene, the high polymer concentrations is prerequisite for formation of stable jet during electrospinning. Stable jet should reduce the number of beads (defects) significantly. As stated earlier, the spinnability of AXyl_PVA$_7$ system with increase of arabinoxylan concentration to 10 wt% was impossible due to too high viscosity of the solution. Based on the results of this work, it is preferred to increase the concentration of polymers and use of higher temperatures to improve the spinnability of solution and to obtain defect-free fibres.

Chemical composition of nanofibrous mats

The FT-IR spectroscopy was used to assess the chemical composition of the electrospun mats, and the spectra have been presented in Fig. 11. In order to interpret the FT-IR spectra of the electrospun mats, the spectra of pure powders of PVA, arabinoxylan extracted from barley husk and xylan extracted from beechwood were measured and peak assignments have been shown in Table 5.

Following conclusions were drawn based on data shown in Table 5. First, the main difference between spectra of xylan and arabinoxylan is absence of peaks at 1510 and 1595 cm^{-1} which can be assigned to the aromatic skeletal vibrations of lignin residue (Sun et al. 2005). Second, the common features for xylan and arabinoxylan are peaks associated with xylopyranose backbone: peak at 1035–1041 cm^{-1}, which is attributed to the C–O stretching, peaks at 2919 cm^{-1} and 3341–3343 cm^{-1} assigned to C–H and O–H stretching, respectively (Duan et al. 2019). The peak at 1035–1041 cm^{-1} in xylans has two shoulders at 1160 and 987 cm^{-1} of low-intensity. The peak

Table 5 The main bands identified on FT-IR spectra of Xyl, AXyl and PVA powders

Wavenumbers for Xyl (cm^{-1})	Wavenumbers for AXyl (cm^{-1})	Wavenumbers for PVA (cm^{-1})
987	987	916
1041	1035	1086
1160	1160	1142
1250	1252	1238
1377	1377	1378
1408	1414	1418
	1510	
1603	1595	1650
2919	2919	2940
3343	3341	3272

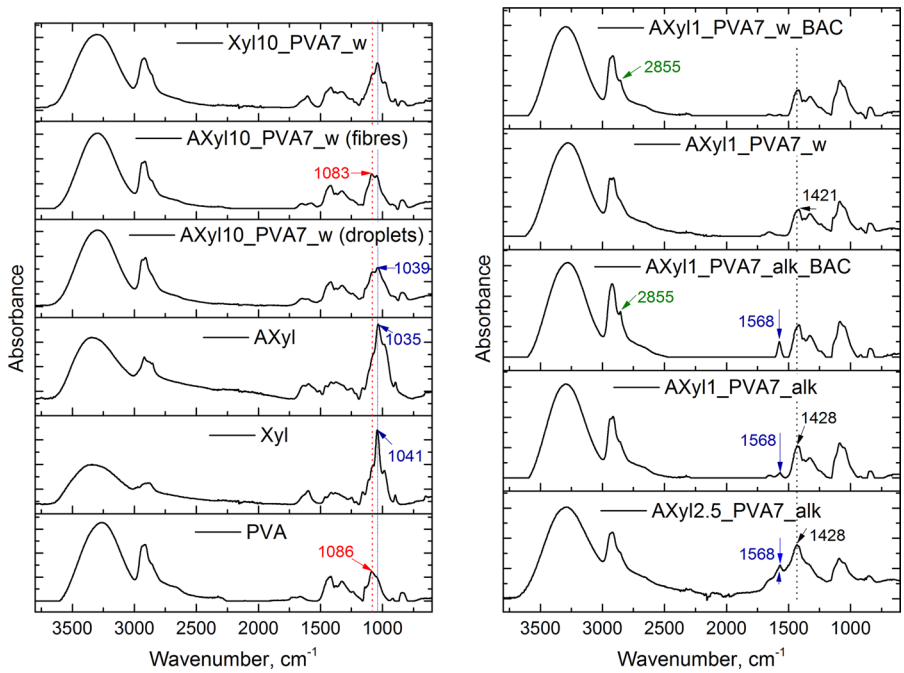

Fig. 11 FT-IR spectra of studied electrospun mats and reference components: PVA, xylan and arabinoxylan powders

at 1603 cm^{-1} in xylan spectra can be explained by absorbed water. In general, the spectra of xylans and PVA are close to each other, for example the peaks 1377–1378, 1414–1418 and 1252–1238 cm^{-1} corresponding to the C–H and C–O stretching and bending vibrations in xylans and PVA molecules (Sun et al. 2005; Bary et al. 2019). The characteristic peak of PVA at 1086 cm^{-1} has shoulder at 1142 cm^{-1}, which determines polymer crystallinity (Mallapragada et al. 1996, Tretinnikov et al. 2012). There are differences between the xylan and PVA peaks obtained in region above 2000 cm^{-1}. The peaks at 3272 and 2940 cm^{-1} correspond to O–H and C–H stretching of PVA, respectively.

Analysis of spectra of $AXyl_{10}$_PVA_7_w droplets and fibres showed that fibres had more pronounced peak at 1083 cm^{-1} that is closer to the characteristic peak of PVA, while droplets had more pronounced peak at 1039 cm^{-1} and no peak at 1083 cm^{-1}. Use of alkaline for arabinoxylan dissolution caused the formation of the peaks at 1434 and 1565–1574 cm^{-1}. They are considered as shifts from peaks with original positions 1421 and 1595 cm^{-1} which correspond to aromatic skeletal vibrations. It is known that in an alkaline solution, ionization of the phenolic hydroxyl groups is responsible for the shifts of the phenolic absorption bands of compounds (Morohoshi 1991). The arabinoxylan extract from barley husks contained 19.6% of Klason lignin. Lignin was thought to be a reason why AXyl formed the dispersion in water. Addition of surfactant to the $AXyl_1$_PVA_7_w and $AXyl_1$_PVA_7_alk solutions was appeared as a sharp peak at 2855 cm^{-1}, which is typical for benzalkonium chloride.

Hydrophilicity of electrospun mats

Contact angles of the electrospun mats as a function of composition has been shown in Table 6, where the mean values and standard deviations have been calculated out of 15 (3 × 5) measurements. Two-sample t-test and Tukey's simultaneous test were applied to determine if changes in contact angle from the PVA_7_w was statistically significant at P-value less than 0.05.

The contact angle measurements are very sensitive to roughness and porosity of surface. The difference in microstructure of spun mats can be assessed from SEM images presented in earlier section. As can be seen, equal times (means equal fused volumes) of spinning was not warranty that fibre mats produced had similar microstructure (i.e., porosity). As can be seen from Table 6, the contact angle of Xyl_{10}_PVA_7_w mat was significantly lower than the contact angle of PVA_7_w and $AXyl_{10}$_PVA7_w mats. Hydrophilic nature of former mat can be explained by hydrophilicity of beechwood xylan. Presence of lignin in extract of arabinoxylan can explain its higher hydrophobicity. Decrease in content of arabinoxylan extract (from 10 to 1 wt%) and consequently in lignin concentration led to predictable decrease in hydrophobicity of mat. Usage of alkaline for arabinoxylan dissolution led to formation of highly hydrophilic mats. This hydrophilicity is in a good agreement with results of FTIR analysis which revealed ionization of the phenolic hydroxyl groups of lignin at alkaline conditions.

Table 6 Contact angles of electrospun mats

Sample	Contact angle (°)	Trend
PVA_7_w	46.9 ± 8.4	Reference
Xyl_{10}_PVA_7_w	30.2 ± 5.1	↓ (S)
$AXyl_{10}$_PVA_7_w	54.3 ± 6.2	↑ (NS)
$AXyl_1$_PVA_7_w	48.1 ± 2.2	↑ (NS)
$AXyl_1$_PVA_7_alk	18.0 ± 3.0	↓ (S)

S corresponds to significant change (at probability level 0.05), NS corresponds to non-significant change (at probability level 0.05), and arrows show the trends (↑ corresponds to improvement and ↓ corresponds to decline)

Conclusion

This study was focused on the spinnability of the arabinoxylan extracted from barley husk. Two different solvents were applied to produce the spinning solutions. It was found that alkaline conditions were required to solubilize the arabinoxylan extract. Among other components of the arabinoxylan extract, lignin was believed to be a major one to determine solubility. In contrast to the arabinoxylan extract, the xylan extracted from beechwood was easily soluble in hot water. The comparison of flow consistency indexes, *K*, of Xyl_{10}_PVA_7_w and $AXyl_{10}$_PVA_7_w solutions (5.322 v's 44.11) clearly showed that the former solution was less viscous. Moreover, the Xyl_{10}_PVA_7_w solution had

improved spinnability compared to the $AXyl_{10}$–PVA_7_w solution. The higher viscosity of the $AXyl_{10}$_PVA_7_w solution can be explained by higher molar mass of arabinoxylan and presence of lignin in arabinoxylan extract. Decrease in viscosity of the AXyl_PVA solutions was achieved by decreasing the concentration of the arabinoxylan. The spinnability of the less viscous $AXyl_1$_PVA_7_w solution (K of 0.157) was improved compared to the $AXyl_{10}$_PVA_7_w solution.

In addition, lignin was found to be responsible for increased hydrophobicity nanofibrous mats; the values of contact angle were determined as 30.2° and 54.3° for $Xy1_{10}$_PVA_7_w and $AXy1_{10}$_PVA_7_w mats, respectively. In future studies, the lignin-rich solution can be used to improve the water resistance of the PVA-based nanofibres. However, when comparing the $AXyl_1$_PVA_7_w and $AXyl_1$_PVA_7_alk mats having contact angles 48.1° and 18°, respectively, it became obvious that solvent nature can also drastically change the hydrophilicity of the mats.

The rheological measurements demonstrated clearly that the type of solvent was the key factor affecting the interaction between polymers (i.e., PVA and arabinoxylan/lignin) and surfactants. However, more work is needed to understand the interactions between molecules and molecular structure of the nanofibrous mats. The 75–200 nm fibres electrospun in this study have potential applications in the fields where high aspect ratio (or high surface area) of fibres is required (e.g., air filtration).

Acknowledgements This study was supported by the Business Finland funded BioProt Co-creation project (1.7.2020-28.2.2021), which aimed on development of bio-based and biodegradable nonwoven materials from forest industry and use as protective equipment. Authors are thankful to Prof. Kristiina Oksman and Dr. Linn Berglund from the Laboratory of Wood and Bionanocomposites, Luleå, Sweden for supply of arabinoxylan extract.

Author contributions SB designed, performed most of experiments, analyzed the data, and wrote the manuscript; KK characterized properties of solutions, and wrote the manuscript; SH revised the manuscript; KL obtained the funding and revised the manuscript.

Funding Open Access funding provided by LUT University (previously Lappeenranta University of Technology (LUT)). This study was mainly supported by the Business Finland funded BioProt Co-creation project (1.7.2020–28.2.2021), which aimed on development of bio-based and biodegradable nonwoven materials from forest industry and use as protective equipment. Additional funding was obtained as a grant awarded by Etelä-Karjalan Säästöpankkisäätiö to Dr. Katri Laatikainen.

Data availability The corresponding author will provide the datasets generated for this study on request.

Declarations

Conflict of interest The authors declare that they have no known competing financial interests or personal relationships that could have appeared to influence the work reported in this paper.

Ethics approval Not applicable.

References

Abdullah Shukry NA, Sekak KA, Ahmad MR and Bustami Effendi TJ (2014) Characteristics of electrospun PVA-Aloe vera nanofibres produced via electrospinning. In: Proceedings of the international colloquium in textile engineering, fashion, apparel and design 2014 (ICTEFAD 2014). Ed(s) Ahmad MR and Yahya MF, Springer, pp 7–12. https://doi.org/10.1007/978-981-287-011-7_2

Agarwal S, Greiner A, Wendorff JH (2009) Electrospinning of manmade and biopolymer nanofibers - Progress in techniques, materials, and applications. Adv Funct Mater 19:2863–2879. https://doi.org/10.1002/adfm.200900591

Agarwal S, Burgard M, Greiner A, Wendorff JH (2016) Electrospinning—a practical guide to nanofibers. De Gruyter, Berlin, Boston. https://doi.org/10.1515/9783110333510

Ago M, Jakes JE, Johansson L-S, Park S, Rojas OJ (2012) Interfacial properties of lignin-based electrospun nanofibers and films reinforced with cellulose nanocrystals. ACS Appl Mater Inter 4:6849–6856. https://doi.org/10.1021/am302008p

Bary EMA, Fekry A, Soliman YA, Harmal AN (2019) Characterisation and swelling-deswelling properties of superabsorbent membranes made of PVA and cellulose nanocrystals. Int J Environ Stud 76:118–135. https://doi.org/10.1080/00207233.2018.1496607

Berglund L, Forsberg F, Jonoobi M, Oksman K (2018) Promoted hydrogel formation of lignin-containing arabinoxylan aerogel using cellulose nanofibers as a functional biomaterial. RSC Adv 8:38219–38228. https://doi.org/10.1039/C8RA08166B

Bhardwaj A, Alam T, Sharma V, Alam MS, Hamid H, Deshwal GK (2020) Lignocellulosic agricultural biomass as a biodegradable and eco-friendly alternative for polymer-based food packaging. J Package Technol Res 4:205–216. https://doi.org/10.1007/s41783-020-00089-7

Börjesson M, Härdelin L, Nylander F, Karlsson K, Larsson A, Westman G (2018) Arabinoxylan and nanocellulose from a kilogram-scale extraction of barley husk. BioResources 13(3):6201–6220. https://doi.org/10.15376/biores.13.3.6201-6220

Duan J, Karaaslan MA, MiJ C, Li-Y L, Johnson AM, Renneckar S (2019) Investigation into electrospinning water-soluble xylan: developing applications from highly absorbent and hydrophilic surfaces to carbonized fiber. Cellulose 26:413–427. https://doi.org/10.1007/s10570-018-2188-2

Ebringerová A (2006) Structural diversity and application potential of hemicelluloses. Macromol Symp 232:1–12. https://doi.org/10.1002/masy.200551401

Ebringerová A, Heize T (2000) Xylan and xylan derivatives-biopolymers with valuable properties, 1 Naturally occuring xylan structures, isolation procedures and properties. Macromol Rapid Commun 21(9):542–556

FAOSTAT, Food and agriculture organization of the United Nations: http://www.fao.org/faostat/. Read 5.1.2021

Ferrari E, Ranucci E, Edlund U, Albertsson AC (2015) Design of renewable poly(amidoamine)/hemicellulose hydrogels for heavy metal adsorption. J Appl Polym Sci 132:41695. https://doi.org/10.1002/app.41695

Forni S (2020) European Commission, European policy on biobased, biodegradable, and compostable plastics. 16 p. https://lab.fi/sites/default/files/2020-12/Biobased%20%26%20Biodegradable%20Plastics_Silvia%20Forni.pdf. Accessed 20 Nov 2021

Frenot A, Chronakis IS (2003) Polymer nanofibers assembled by electrospinning. Curr Opin Colloid in 8:64–75. https://doi.org/10.1016/s1359-0294(03)00004-9

Glasser WG, Kaar WE, Jain RK, Sealey JE (2000) Isolation options for non-cellulosic heteropolysaccharides (HetPS). Cellulose 7:299–317. https://doi.org/10.1023/A:1009277009836

Gröndahl M, Bindgård L, Gatenholm P, Hjertberg T (2014) US Pat. 2014/0093724A1

Handbook of Pharmaceutical Excipients. Rowe RC, Sheskey PJ, Owen SC (Eds) (2006) Pub. Pharmaceutical press and the American pharmacists association. p 61–63

Holmberg K, Jönsson B, Kronberg B, Lindman B (2002) Surfactant-polymer systems. In: Holmberg K, Jönsson B, Kronberg B, Lindman B (eds) Surfactants and polymers in aqueous solution. Wiley, pp 277–303

Holopainen-Mantila U (2015) Composition and structure of barley (*Hordeum vulgare L.*) grain in relation to end uses. Doctoral Thesis, University of Helsinki. Published in VTT Science 78 series, p 108. ISSN 2242–1203

Höije A, Gröndahl M, Tømmeraas K, Gatenholm P (2005) Isolation and characterization of physicochemical and material properties of arabinoxylans from barley husks. Carbohyd Polym 6:266–275

Höije A, Sandström C, Roubroeks JP, Andersson R, Gohil S, Gatenholm P (2006) Evidence of the presence of 2-O-b-D-xylopyranosyl-a-L-arabinofuranose side chains in barley husk arabinoxylan. Carbohyd Res 341:2959–2966. https://doi.org/10.1016/j.carres.2006.10.008

Jain RK, Sjöstedt M, Glasser WG (2001) Thermoplastic xylan derivatives with propylene oxide. Cellulose 7:319–336. https://doi.org/10.1023/A:1009260415771

Jarusuwannapoom T, Hongrojjanawiwat W, Jitjaicham S, Wannatong L, Nithitanakul M, Pattamaprom C, Koombhongse P, Rangkupan R, Supaphol P (2005) Effect of solvents on electro-spinnability of polystyrene solutions and morphological appearance of resulting electrospun polystyrene fibres. Eur Polym J 41:409–421. https://doi.org/10.1016/j.eurpolymj.2004.10.010

Krishnan R, Rajeswari R, Venugopal J, Sundarrajan S, Sridhar R, Shayanti M, Ramakrishna S (2012) Polysaccharide nanofibrous scaffolds as a model for in vitro skin tissue regeneration. J Mater Sci 23:1511–1519. https://doi.org/10.1007/s10856-012-4630-6

Kumar M, Hietala M, Oksman K (2019) Lignin-based electrospun carbon nanofibres. Front Mater. https://doi.org/10.3389/fmats.2019.00062

Köhnke T, Brelid H, Westman G (2009) Adsorption of cationized barley husk xylan on kraft pulp fibres: influence of degree of cationization on adsorption characteristics. Cellulose 16:1109–1121. https://doi.org/10.1007/s10570-009-9341-x

Lai Y-Z (1991) Chemical degradation. In: Hon DN-S, Shiraishi N (eds) Wood and cellulosic chemistry. Marcel Dekker Inc, New York, pp 455–523

Lee KH, Kim HY, Bang HJ, Jung YH, Lee SG (2003) The change of bead morphology formed on electrospun polystyrene fibres. Polymer 44:4029–4034. https://doi.org/10.1016/s0032-3861(03)00345-8

Lin T, Wang H, Wang H, Wang X (2004) The charge effect of cationic surfactants on the elimination of fibre beads in the electrospinning of polystyrene. Nanotechnology 15:1375–1381. https://doi.org/10.1088/0957-4484/15/9/044

Luke, https://www.luke.fi/ruokafakta/en/field-crops/grain-production-volumes/. Read 5.1.2021

Lähde A, Haluska O, Alatalo SM, Sippula O, Meščeriakovas A, Lappalainen R, Nissinen T, Riikonen J, Lehto VP (2020) Synthesis of graphene-like carbon from agricultural side stream with magnesiothermic reduction coupled with atmospheric pressure induction annealing. Nano Express 1(010014):9p

Mallapragada SK, Peppas NA (1996) Dissolution mechanism of semicrystalline poly(vinyl alcohol) in water. J Polym Sci: Part B 34:1339–1346

Mewis J, Wagner NJ (2011) Introduction to colloid science and rheology. In: Mewis J, Wagner NJ (eds) Colloidal Suspension Rheology. Cambridge University Press, Cambridge, pp 1–35

Moohan J, Stewart SA, Espinosa E, Rosal A, Rodríguez A, Larrañeta E, Donnelly RF, Domínguez-Robles J (2019) Cellulose nanofibers and other biopolymers for biomedical application. Rev Appl Sci 10(1):65. https://doi.org/10.3390/app10010065

Morohoshi N (1991) Chemical characterization of wood and its components. In: Hon DN-S, Shiraishi N (eds) Wood and cellulosic chemistry. Marcel Dekker Inc, New York, pp 331–392

Nygren C (2009) Recovery of chemicals in xylan extraction process. Master of Science Thesis, Linköping University

Park JH, Lee HW, Chae DK, Oh W, Yun JD, Deng Y, Yeum JH (2009) Electrospinning and characterization of poly(vinyl alcohol)/chitosan oligosaccharide/clay nanocomposite nanofibers in aqueous solutions. Colloid Polym Sci 287:943–950. https://doi.org/10.1007/s00396-009-2050-z

Peng F, Guan Y, Zhang B, Bian J, Ren J-Li, Yao C-Li (2014) Synthesis and properties of hemicellulose-based semi-IPN hydrogels. Int J Biol Macromol 65:564–572. https://doi.org/10.1016/j.ijbiomac.2014.02.003

Peresin MS, Rojas OJ (2014) Electrospinning of nanocellulose-based materials. In: Oksman K, Mathew AP, Bismarck A, Rojas O, Sain M (eds) Handbook of green Materials. World Scientific, New Jersey, pp 163–183. https://doi.org/10.1142/9789814566469_0041

Ristolainen N, Heikkilä P, Harlin A, Seppälä J (2006) Poly(vinyl alcohol) and polyamide-66 nanocomposites prepared by electrospinning. Macromol Mater Eng 291(2):114–122. https://doi.org/10.1002/mame.200500213

Rogina A (2014) Electrospinning process: Versatile preparation method for biodegradable and natural polymers and biocomposite systems applied in tissue engineering and drug delivery. Appl Surf Sci 296:221–230. https://doi.org/10.1016/j.apsusc.2014.01.098

Roos AA, Persson T, Krawczyk H, Zacchi G, Stålbrand H (2009) Extraction of water-soluble hemicelluloses from barley husks. Bioresource Technol 100:763–769. https://doi.org/10.1016/j.biortech.2008.07.022

Sjöström E (1989) The origin of charge of cellulosic fibers. Nordic Pulp Pap Res J 4(2):90–93. https://doi.org/10.3183/nppj-1989-04-02-p090-093

Subbiah T, Bhat Tock GSRW, Parameswaran S, Ramkumar SS (2005) Electrospinning of Nanofibers. J Appl Polym Sci 96:557–569. https://doi.org/10.1002/app.21481

Sun XF, Sun RC, Fowler P, Baird MS (2005) Extraction and characterisation of original lignin and hemicelluloses from wheat straw. J Agric Food Chem 53:860–870. https://doi.org/10.1021/jf040456q

Sun XF, Jing Z, Fowler P, Wu Y (2011) Rajaratnam M. Structural characterisation and isolation of lignin and hemicelluloses from barley straw. Ind Crops Prod 33:588–598

Teleman A, Tenkanen M, Jacobs A, Dahlman O (2002) Characterization of O-acetyl- (4-O methylglucurono)xylan isolated from birch and beech. Carbohyd Res 337(4):373–377. https://doi.org/10.1016/S0008-6215(01)00327-5

Torres-Giner S, Wilkanowicz S, Melendez-Rodriguez B, Lagaron JM (2017) Nanoencapsulation of aloe vera in synthetic and naturally occurring polymers by electrohydrodynamic processing of interest in food technology and bioactive packaging. J Agric Food Chem 65:4439–4448. https://doi.org/10.1021/acs.jafc.7b01393

Torres-Giner S, Busolo M, Cherpinski A, Lagaron JM (2018) Electrospinning in the packaging industry. In: Kny E, Ghosal K, Thomas S (eds) Electrospinning - from basic research to commercialization. Royal Society of Chemistry, London, pp 238–260

Tretinnikov ON, Zagorskaya SA (2012) Determination of the degree of crystallinity of poly(vinyl alcohol) by FTIR spectroscopy. J Appl Spectrosc 79:521–526. https://doi.org/10.1007/s10812-012-9634-y

Turku I, Sainio T (2009) Modelling of adsorptive removal of benzalkonium chloride from water with a polymeric adsorbent. Sep Purif Technol 69:185–194. https://doi.org/10.1016/j.seppur.2009.07.017

Uyar T, Besenbacher F (2008) Electrospinning of uniform polystyrene fibres: the effect of solvent conductivity. Polymer 49:5336–5343. https://doi.org/10.1016/j.polymer.2008.09.025

Venugopal J, Rajeswari R, Shayanti M, Sridar R, Sundarrajan S, Balamurugan R, Ramakrisha S (2013) Xylan polysaccharides fabricated into nanofibrous substrate for myocardial infarction. Mater Sci Eng C 33:1325–1331. https://doi.org/10.1016/j.msec.2012.12.032

Wang C, Li Y, Ding G, Xie X, Mianheng J (2012) Preparation and characterization of graphene oxide/poly(vinyl alcohol) composite nanofibers via electrospinning. J Appl Polym Sci 127(4):3026–3032. https://doi.org/10.1002/app.37656

Yao L, Haas TW, Guiseppi-Elie A, Bowlin GL, Simpson DG, Wnek GE (2003) Electrospinning and stabilization of fully hydrolysed poly(vinyl alcohol) fibres. Chem Mater 15:1860–1864. https://doi.org/10.1021/cm0210795